










7<sup>th</sup> INTERNATIONAL WORKSHOP ON NEW PHOTON-DETECTOR  
BOLOGNA, ITALY  
3–5 DECEMBER 2025

## Radiation hardness characterization of silicon photomultipliers for next-generation particle identification detectors

B. Gardinovački <sup>a,b,\*</sup> D.C. Rodríguez <sup>a</sup> R. Dolenc <sup>b,a</sup> T.M. Drozdek,<sup>a</sup> P. Križan <sup>b,a</sup>  
S. Korpar <sup>c,a</sup> A. Seljak <sup>a</sup> A.G. Gola <sup>d</sup> M. Penna,<sup>d</sup> F. Acerbi <sup>d</sup> and R. Pestotnik <sup>a</sup>

<sup>a</sup>Experimental Particle Physics Department, Jožef Stefan Institute,  
Jamova cesta 39, Ljubljana, 1000, Slovenia

<sup>b</sup>Faculty of Mathematics and Physics, University of Ljubljana,  
Jadranska ulica 19, Ljubljana, 1000, Slovenia

<sup>c</sup>Faculty of Chemistry and Chemical Engineering, University of Maribor,  
Smetanova ulica 17, Maribor, 2000, Slovenia

<sup>d</sup>Fondazione Bruno Kessler,  
Via Sommarive 18, Trento, 38123, Italy

E-mail: [boris.gardinovacki@ijs.si](mailto:boris.gardinovacki@ijs.si)

**ABSTRACT.** Silicon photomultipliers (SiPMs) are promising candidates for the new photon detectors of the Ring Imaging Cherenkov (RICH) detector in the LHCb experiment at CERN. With the increased luminosity of the High-Luminosity LHC, the RICH photon detector must be upgraded to handle higher photon overlap and improved spatial granularity, while also withstanding greater doses of radiation. The radiation tolerance of SiPMs remains a key challenge for their use in high-energy physics, motivating extensive research. This work investigates the effects of cryogenic temperatures on single-photon detection in neutron-irradiated SiPMs based on NUV-HD-MT (metal-in-trench) technology, using low-field, and ultra-low-field variants. The results demonstrate that cryogenic cooling can mitigate the impact of neutron induced damage at fluences up to  $1 \times 10^{12} n_{\text{eq}}/\text{cm}^2$  and recover the single-photon resolution.

**KEYWORDS:** Photon detectors for UV, visible and IR photons (solid-state); Radiation-hard detectors; Cryogenic detectors; Radiation damage to detector materials (solid state)

\*Corresponding author.

---

## Contents

<b>1</b>	<b>Introduction</b>	<b>1</b>
<b>2</b>	<b>Experimental setup</b>	<b>1</b>
<b>3</b>	<b>Results</b>	<b>3</b>

---

## 1 Introduction

Silicon photomultipliers (SiPMs) are light detectors used in many applications that require single-photon counting and precise timing. The Ring Imaging Cherenkov detector (RICH) at the LHCb experiment will be upgraded during Upgrade 2 of the Large Hadron Collider to operate at the higher instantaneous luminosity of the High Luminosity LHC (HL-LHC) [1]. This requires a new photon detection system with improved time resolution for single photons. SiPMs are an attractive option due to their fast timing and high spatial granularity [2]. However, their main limitation is low tolerance to ionizing radiation. Radiation damage (i) reduces the separation between photon signals arriving close in time, (ii) makes it increasingly difficult to distinguish true photon signals from dark counts, and (iii) degrades the proportionality between signal height and the number of detected photons [3, 4]. The goal of this work is to investigate the effects of temperature and neutron irradiation on the performance of SiPMs, particularly focused on the recovery of the single-photon detection resolution, which is typically lost due to the high level of primary dark count rate after irradiation.

The samples used in this characterization run are designed and produced by Fondazione Bruno Kessler (FBK, Trento, Italy). They are based on NUV-HD-MT (metal-in-trench) technology [5], with variants as low-field (LF) and ultra-low-field (ULF), which differ in the peak electric field value in the avalanche multiplication region. Thanks to the metal filled trench between microcells the optical crosstalk is significantly reduced, while keeping all other performance parameters of the NUV-HD technology, e.g. low noise and detection efficiency peaked in the blue and NUV part of the spectrum. All samples have a 40  $\mu\text{m}$  cell pitch and  $1 \times 1 \text{ mm}^2$  active surface area. For each technology, three samples were tested, two of which were irradiated.

They were irradiated by neutrons at the TRIGA reactor of the Jožef Stefan Institute in Ljubljana. The chosen fluences were  $1 \times 10^{10}$  and  $1 \times 10^{12} n_{\text{eq}}/\text{cm}^2$ , where  $n_{\text{eq}}$  denotes the 1 MeV neutron-equivalent fluence. After irradiation, the samples were annealed for 80 minutes at 60  $^\circ\text{C}$ .

## 2 Experimental setup

The measurement setup is centered around an insulated, dry liquid nitrogen container and is an upgrade of the setup used in [6]. A metal, experimental box shown in figure 1 is lowered into the cryogenic container. The inside of the container is kept at liquid nitrogen temperature while the inside of the box, due to insulating material stays at  $-180^\circ\text{C}$ . Higher temperatures for measurement are achieved with resistive heaters that are attached to the side of the box. Thermal paste provides proper thermal contact to the temperature sensor and the SiPM samples through their pins.

Inside the box are the SiPM sample, a temperature sensor, and an amplifier electronics board. The electronic circuit is used for bias voltage smoothing, signal filtering, and amplification of the SiPM signal. Illumination is provided by fast-triggered Alphalas PLDD-20M driver and Picopower

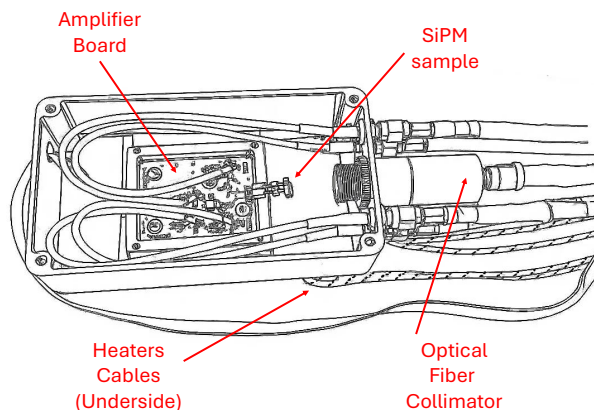


**Figure 1.** RF-shielded experimental box that contains the SiPM sample plugged into the amplifier board and the cable connections to the measuring instruments.

LD-405 laser with 405 nm wavelength and 100 kHz repetition frequency. The bias voltage and current measurements are done using a Keithley 6517B electrometer, while signal acquisition is performed with a Teledyne LeCroy HDO6104b oscilloscope with 1 GHz bandwidth and 10 GS/s sampling rate. Capacitance measurements are carried out using an OWON LCR2000 meter connected to the board through decoupling capacitors to protect the instrument from the high bias voltage.

195,000 events are acquired using the sequence mode of the oscilloscope, during which the environmental parameters remain stable. Data is collected for each SiPM sample at six temperatures from  $-180^{\circ}\text{C}$  to  $20^{\circ}\text{C}$  and five over-voltage values. An event consists of a 100 ns waveform containing a laser pulse for triggering and illumination and the SiPM response signal, shown in figure 2 (left). This study focuses on single-photon detection performance, so events were classified by pulse peak height, which proved cleaner than the traditional charge spectrum. Figure 2 (right) shows the histogram of pulse peak heights used for single-hit event selection.

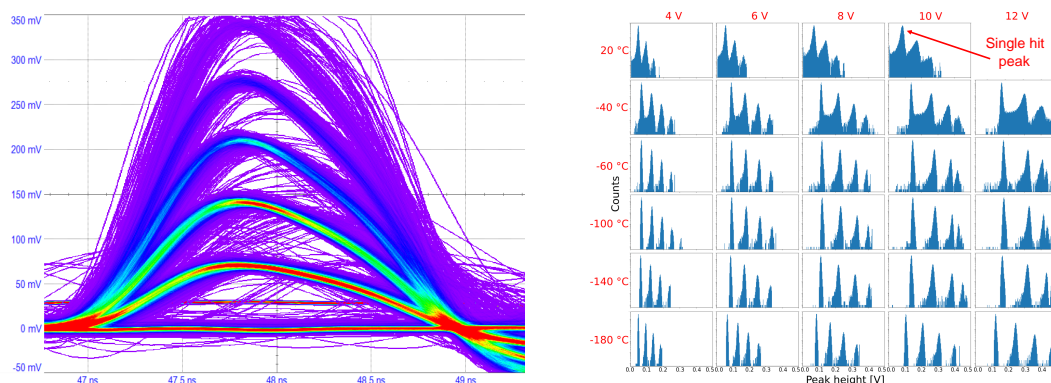
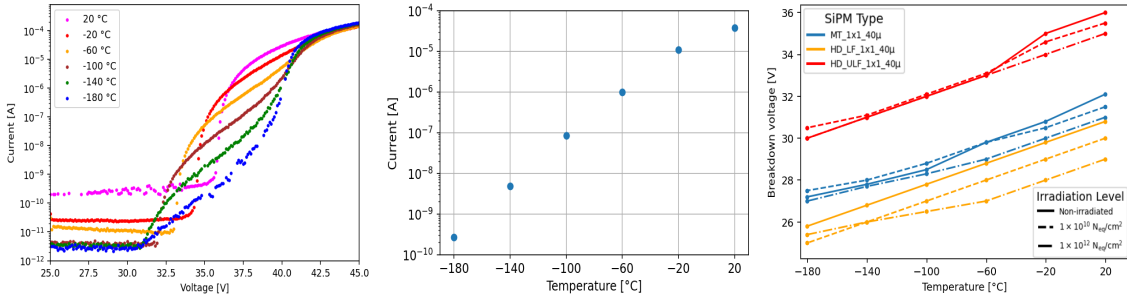


**Figure 2.** Oscilloscope view of accumulated events showing clear separation of detected photon numbers. The light intensity was adjusted to maximize single-photon events (left). Peak height spectra for different temperatures and over-voltages for the MT-1x1-40 $\mu$  sample irradiated at a neutron fluence of  $1 \times 10^{10} n_{\text{eq}}/\text{cm}^2$  (right). The single-hit peaks correspond to the leftmost peaks in the spectra. The  $20^{\circ}\text{C}$ , 12 V measurement is omitted because the light peaks could not be distinguished from noise.

### 3 Results

The same measurements were performed for all SiPM samples to study the effects of temperature, neutron irradiation, and technology on single-photon detection performance. Results are presented for temperatures from  $-180\text{ }^{\circ}\text{C}$  to  $20\text{ }^{\circ}\text{C}$  and neutron fluences of  $1 \times 10^{10}\text{ }n_{\text{eq}}/\text{cm}^2$  and  $1 \times 10^{12}\text{ }n_{\text{eq}}/\text{cm}^2$ .

Figure 3 (left) shows the reverse bias current-voltage (I-V) characteristics of the SiPM sample HD-ULF-1x1-40 $\mu$  irradiated with  $1 \times 10^{10}\text{ }n_{\text{eq}}/\text{cm}^2$ . The dark current decreases with decreasing temperature. Cooling also reduces the breakdown voltage: a temperature decrease of approximately  $40\text{ }^{\circ}\text{C}$  lowers the breakdown voltage by about 1 V (right). The breakdown voltage is determined from the maximum of the second derivative of the logarithmic reverse bias I-V curve.



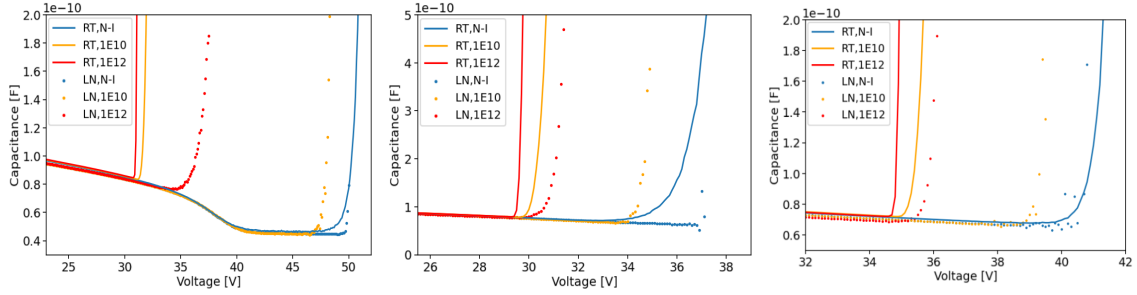
**Figure 3.** Current-voltage characteristic of HD-ULF-1x1-40 $\mu$  sample irradiated to  $1 \times 10^{10}\text{ }n_{\text{eq}}/\text{cm}^2$  for different temperatures (left). A clear decrease in the dark current can be observed for lower temperatures at a fixed over-voltage of 5 V (center). Effects of temperature and radiation on the breakdown voltage for all the samples are shown on the right.

Table 1 shows the effect of cooling and irradiation on the SiPM resistance, extracted from the slope of the linear part of the forward I-V curve. The resistance uncertainties were calculated from the error of the fit.

**Table 1.** SiPM resistance  $R$  for different SiPM types, irradiation fluences, and temperatures.

SiPM Type	Fluence ( $n_{\text{eq}}/\text{cm}^2$ )	$R$ (20 °C) [k $\Omega$ ]	$R$ (-180 °C) [k $\Omega$ ]	$\Delta R$ [k $\Omega$ ]
MT	Non-irradiated	3.6	6.9	0.2
MT	$1 \times 10^{10}$	1.8	7.9	0.2
MT	$1 \times 10^{12}$	2.0	8.4	0.2
LF	Non-irradiated	3.5	8.3	0.2
LF	$1 \times 10^{10}$	2.0	10.1	0.2
LF	$1 \times 10^{12}$	1.9	9.9	0.2
ULF	Non-irradiated	3.7	10.9	0.2
ULF	$1 \times 10^{10}$	2.1	11.3	0.2
ULF	$1 \times 10^{12}$	2.5	10.9	0.2

Capacitance-Voltage (C-V) measurements were performed to determine the full-depletion voltage of the SiPMs and study the effect of irradiation, shown in figure 4. With our setup, only the MT samples showed a resolvable full-depletion voltage. For the other samples, the curves exhibit abnormal behavior at higher voltages. Cooling extends the measurable range but does not allow reaching full depletion. Further investigation is needed to understand this behavior.



**Figure 4.** Capacitance-Voltage plots for MT (left), LF (middle) and ULF (right) variant measured at room temperature (RT, solid line) and  $-180^{\circ}\text{C}$  (LN, dotted line). Plots show curves corresponding to non-irradiated samples (N-I) and samples irradiated with  $1 \times 10^{10}$  and  $1 \times 10^{12} n_{\text{eq}}/\text{cm}^2$ .

Timing analysis was performed on the waveforms. Single-photon events were selected, and the time-of-arrival (ToA) and time-over-threshold (ToT) were determined for each event. As shown in figure 5 (left), histograms of the ToAs were fitted with an exponentially modified Gaussian, from which the full-width at half-maximum (FWHM) was extracted. Figure 5 (middle) shows the FWHM as a function of the threshold, expressed both in voltage and as a percentage of the full peak height. A characteristic minimum was observed between 20% and 40% of the average single-hit pulse height, for all measurements, and a threshold of 30% was chosen for the subsequent analysis. The rightmost plot shows the effect of temperature on the FWHM of ToAs for different over-voltages.

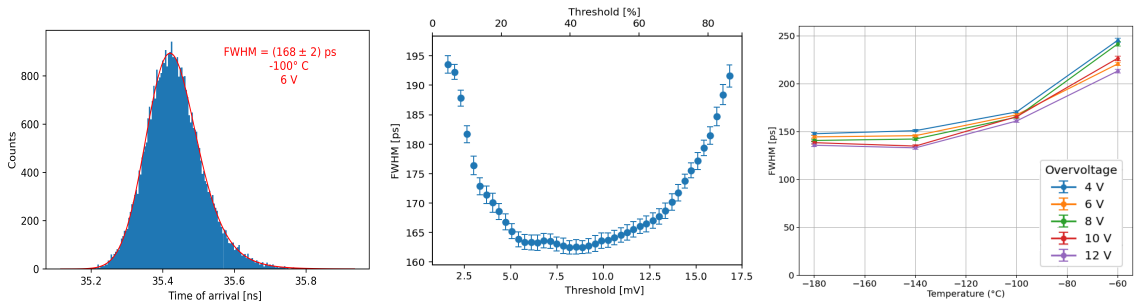


**Figure 5.** Timing analysis of the HD-LF-1x1-40  $\mu\text{m}$  irradiated at  $1 \times 10^{12} n_{\text{eq}}/\text{cm}^2$ . The left image shows a time-of-arrival distribution fitted with an EMG function, from which the FWHM is extracted. The FWHM uncertainty was estimated using the bootstrapping method [7]. The middle image shows the dependence of FWHM on threshold height, while the right image shows its dependence on temperature and over-voltage. At higher temperatures, the timing analysis was not possible due to excessive noise events.

Separation of events based on the time-over-threshold can be worsened or lost due to radiation damage. Figure 6 shows the degradation of performance in separating events of different heights and merging of histograms with an increase of radiation fluence.

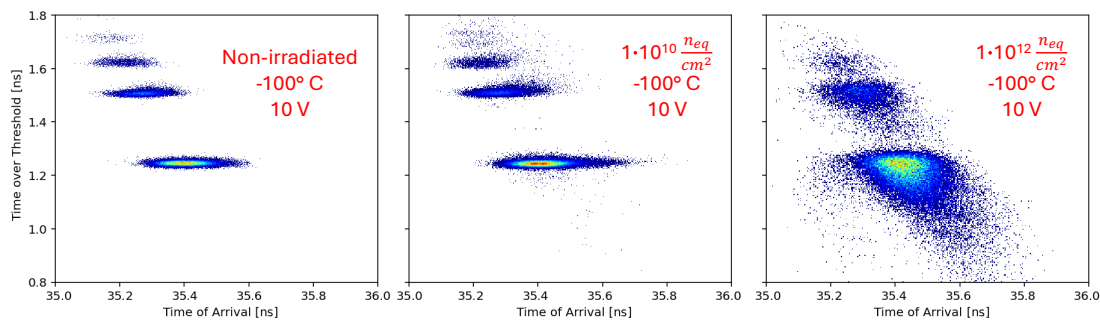


**Figure 6.** Time-over-threshold versus time-of-arrival histogram for the sample MT-1x1-40 $\mu$  at  $-100^\circ\text{C}$  and 10 V over-voltage. The leftmost picture shows the performance of the non-irradiated sample, the middle picture shows the sample at a fluence of  $1 \times 10^{10} n_{\text{eq}}/\text{cm}^2$ , and the rightmost picture corresponds to a fluence of  $1 \times 10^{12} n_{\text{eq}}/\text{cm}^2$ .

## Acknowledgments

We would like to thank the TRIGA nuclear reactor of Jožef Stefan Institute, and the reactor operators for the help with SiPM irradiation. The authors acknowledge the financial support from the AIDAInnova project and the financial support from the Slovenian Research and Innovation Agency (project J1-4358).

## References

- [1] S. Wotton, *The LHCb RICH upgrade for the high luminosity LHC era*, *Nucl. Instrum. Meth. A* **1058** (2024) 168824.
- [2] L.P. Rignanese, P. Antonioli, R. Preghenella and E. Scapparone, *SiPMs and examples of applications for low light detection in particle and astroparticle physics*, *Riv. Nuovo Cim.* **47** (2024) 299.
- [3] E. Garutti and Y. Musienko, *Radiation damage of SiPMs*, *Nucl. Instrum. Meth. A* **926** (2019) 69 [[arXiv:1809.06361](https://arxiv.org/abs/1809.06361)].
- [4] D. Consuegra Rodríguez et al., *Radiation hardness and annealing study of neutron-irradiated silicon photomultipliers*, *2025 JINST* **20** C06033.
- [5] S. Merzi et al., *NUV-HD SiPMs with metal-filled trenches*, *2023 JINST* **18** P05040.
- [6] D. Consuegra Rodríguez et al., *Characterization of neutron-irradiated SiPMs down to liquid nitrogen temperature*, *Eur. Phys. J. C* **84** (2024) 970.
- [7] B. Efron, *Bootstrap Methods: Another Look at the Jackknife*, in *Breakthroughs in Statistics*, Springer (1992), p. 569–593 [[DOI:10.1007/978-1-4612-4380-9\\_41](https://doi.org/10.1007/978-1-4612-4380-9_41)].